

Ruling out Critical Higgs Inflation?

Isabella Masina ^{*1,2,3}

¹Dip. di Fisica e Scienze della Terra, Ferrara University and INFN, Ferrara, Italy

²CP³ - Origins & DIAS, Southern Denmark University, Odense, Denmark

³Theoretical Physics Department, CERN, Geneva, Switzerland

Abstract

We consider critical Higgs inflation, namely Higgs inflation with a rising inflection point at smaller field values than those of the plateau induced by the non-minimal coupling to gravity. It has been proposed that such configuration is compatible with the present CMB observational constraints on inflation, and also with primordial black hole production accounting for the totality or a fraction of the observed dark matter. We study the model taking into account the NNLO corrections to the Higgs effective potential: such corrections are extremely important to reduce the theoretical error associated to the calculation. We find that, in the 3σ window for the relevant low energy parameters, which are the strong coupling and the Higgs mass (the top mass follows by requiring an inflection point), the potential at the inflection point is so large (and so is the Hubble constant during inflation) that the present bound on the tensor-to-scalar ratio is violated. The model is viable only allowing the strong coupling to take its upper $3 - 4\sigma$ value. In our opinion, this tension shows that the model of critical Higgs inflation is likely to be not viable: neither inflation nor black holes as dark matter can be originated in this version of the model.

1 Introduction

It has been recently proposed that critical Higgs inflation is a viable mechanism to produce primordial black holes constituting a fraction or a significant part of the dark matter observed today [1]. This applies in general to potentials with an inflection point followed, at higher field values, by a plateau [2, 3].

Critical Higgs inflation [4–6] is a particular case of Higgs inflation [7, 8], in which the Higgs potential displays a rising inflection point at field values just below the plateau induced by the non-minimal coupling to gravity, ξ . It was introduced with the peculiarity of accounting for quite large, potentially observable, tensor-to-scalar ratio of cosmological perturbations, r , with respect to the standard scenario of Higgs inflation with a large non-minimal coupling ξ , where

*masina@fe.infn.it

r is predicted to be approximately 0.003, together with a scalar tilt of curvature perturbation $n_s \approx 0.97$ [7]. Previous analysis of critical Higgs inflation [4–6] exploited some approximated form for the effective potential, without discussing in detail the theoretical error associated to such approximation: their aim was primarily to show that r could have been large enough to explain the preliminary (and later retired) results of the BICEP collaboration, which were pointing to $r \approx 0.2$ [9].

In critical Higgs inflation, ξ is small enough so that problems related to the violation of unitarity (see e.g. [10]) might be evaded. Recently, it has also been shown that this scenario is safe from the fine tuning associated to the initial conditions [11].

Now that the tensor-to-scalar ratio is better constrained, $r < 0.12$ at 95% C.L. [12,13], and in view of its possible applications in the phenomenology of primordial black holes, it is interesting to have a more robust understanding of the critical Higgs inflation scenario. The aim of this work is precisely to improve the robustness of the predictions of the cosmological observables (like r and n_s), linking them to the present experimental range of the low energy parameters which control the shape of the Higgs effective potential - the strong coupling constant, α_s , the top quark mass, m_t , and the Higgs boson mass, m_H -, and assessing the size of the theoretical error associated to the calculation.

There is general agreement (see [14] and references therein) on the fact that stability of the Standard Model (SM) potential - and so the inflection point configuration - displays a tension with the low energy parameters at about 2σ . More precisely, assuming the theoretical error associated to the Next-to-Next-to-Leading (NNLO) calculation to go in the "right direction", stability requires for instance that α_s , m_t and m_H take respectively their upper 2σ , lower 1σ and central values [14].

In the case of critical Higgs inflation, also the observational constraints on r and n_s have to be fulfilled. The value of the SM Higgs potential at the inflection point, V_i , is particularly important for the prediction of r . Once the low energy parameters are fixed, such value is subject to the theoretical errors associated to the various steps of the calculation: matching, running and effective potential expansion. These errors have been carefully studied in [14]. For instance, it was shown that, even using the RGE-improved tree-level potential at NNLO, a large theoretical error plagues the value of V_i , so that one must consider at least the 1-loop effective potential to obtain a reliable result [14]. The latter work focussed on the case of a rising inflection point in the SM, without any coupling to gravity (namely the possibility of a shallow false vacuum and its applications to cosmology [15–18]). Here we extend the calculation by including the effect of the non-minimal coupling to gravity.

We find that the value of the Higgs potential at the inflection point is higher than what was considered in previous analyses [4–6,11], and whose results were exploited in [1,2] for the issue of black holes. The prediction for r is then accordingly higher. We will show that, even taking into account the NNLO theoretical error, the present upper bound on r can be accommodated only at the price of assuming that α_s takes its upper $3 - 4\sigma$ value¹.

The model of critical Higgs inflation is thus in serious trouble *per se*, and it is quite unrealistic that it might account for a significant fraction of the dark matter seen today under the form of primordial black holes.

The paper is organized as follows. In section 2, following [14], we review how to determine

¹ Notice that the Higgs false vacuum model was ruled out for precisely the same reason [14].

the Higgs potential in the SM according to the present state of the art, and discuss in particular the inflection point configuration. Section 3 is devoted to the model of Higgs inflation, while section 4 discusses the phenomenology of the inflection point configuration in the case of critical Higgs inflation. We draw our conclusions in section 5.

2 Higgs potential in the SM at NNLO

Before introducing the model with the non minimal coupling to gravity, we review the findings of ref. [14] about the rising inflection point configuration of the SM Higgs effective potential, as they will turn out to be relevant also in the case of the non-minimal coupling.

According to our conventions, the potential for the Higgs field ϕ contained in the Higgs doublet $\mathcal{H} = (0 \quad (\phi + v)/\sqrt{2})^T$ is given, at tree-level, by

$$V(\phi) = \frac{\lambda}{6} \left(|\mathcal{H}|^2 - \frac{v^2}{2} \right)^2 \approx \frac{\lambda}{24} \phi^4, \quad (1)$$

where λ is the Higgs quartic coupling, $v = 1/(\sqrt{2}G_\mu)^{1/2} = 246.221$ GeV and G_μ is the Fermi constant from muon decay [19] and the right hand side of eq. (1) holds when considering large field values. Within our normalization, the mass of the Higgs boson and the mass of the fermion f are given by the tree-level relations

$$m_H^2 = \frac{\lambda v^2}{3}, \quad m_f = \frac{h_f v}{\sqrt{2}}, \quad (2)$$

where h_f denotes the associated Yukawa coupling.

In order to extrapolate the behavior of the Higgs potential at very high energies, we adopt the $\overline{\text{MS}}$ scheme and consider the matching and RGE evolution of the relevant couplings which, in addition to the Higgs quartic coupling λ , are: the three gauge couplings g, g', g_3 , the top Yukawa coupling h_t , and the anomalous dimension of the Higgs field γ . We then compute the RGE-improved Higgs effective potential at the Next-to-Next-to-Leading Order (NNLO), that is at the 2-loop level.

Before discussing the procedure associated to matching, running, and effective potential expansion, we review the basic ideas of the RGE: in applications where the effective potential $V_{\text{eff}}(\phi)$ at large ϕ is needed, as is the case for our analysis, potentially large logarithms appears, of the type $\log(\phi/\mu)$ where μ is the renormalization scale, which may spoil the applicability of perturbation theory. The standard way to treat such logarithms is by means of the RGE. The fact that, for fixed values of the bare parameters, the effective potential must be independent of the renormalization scale μ , means that [20]

$$\left(\mu \frac{\partial}{\partial \mu} + \beta_i \frac{\partial}{\partial \lambda_i} - \gamma \frac{\partial}{\partial \phi} \right) V_{\text{eff}} = 0, \quad (3)$$

where

$$\beta_i = \mu \frac{d\lambda_i}{d\mu}, \quad \gamma = -\frac{\mu}{\phi} \frac{d\phi}{d\mu}, \quad (4)$$

are the β -functions corresponding to each of the SM couplings λ_i , and the anomalous dimension of the background field respectively.

The formal solution of the RGE is

$$V_{\text{eff}}(\mu, \lambda_i, \phi) = V_{\text{eff}}(\mu(t), \lambda_i(t), \phi(t)), \quad (5)$$

where

$$\mu(t) = e^t \mu, \quad \phi(t) = e^{\Gamma(t)} \phi, \quad \Gamma(t) = - \int_0^t \gamma(\lambda(t')) dt', \quad (6)$$

and $\lambda_i(t)$ are the SM running couplings, determined by the equation

$$\frac{d\lambda_i(t)}{dt} = \beta_i(\lambda_i(t)), \quad (7)$$

and subject to the boundary conditions $\lambda_i(0) = \lambda_i$. The usefulness of the RGE is that t can be chosen in such a way that the convergence of perturbation theory is improved, which is the case for instance when $\phi(t)/\mu(t) = \mathcal{O}(1)$. In our calculation the boundary conditions are given at the top quark mass, m_t : we will then take $\mu = m_t$ in eq. (6) from now on.

2.1 Matching and running

In order to derive the values of the relevant parameters (g, g', g_3, h_t, λ) at the top pole mass, m_t , we exploit the results of a detailed analysis about the matching procedure, performed by Bednyakov et al. [21]. We refer the interested reader to [21] and [14] for more details; here we just mention our reference values:

- for the strong coupling constant at $m_Z, \alpha_s^{(5)}$: we take the present [22] world average experimental value of the strong coupling constant at $m_Z, \alpha_s^{(5,exp)} = 0.1181$, and its associated 1σ error, $\Delta\alpha_s^{(5,exp)} = 0.0013$;
- for the Higgs mass, m_H : we take the combined ATLAS and CMS result (after Run1) at $1\sigma, m_H^{exp} = 125.09$ GeV and $\Delta m_H^{exp} = 0.24$ GeV [23];
- for the top pole mass, m_t : we take the present combined Tevatron and LHC value of the MC top mass, $m_t^{MC} = (173.34 \pm 0.76)$ GeV [24]; the uncertainty in the identification between the pole and MC top mass is currently estimated to be of order 200 MeV [25, 26] (or even 1 GeV for the most conservative groups [27]).

The β -functions can be organized as a sum of contributions with increasing number of loops:

$$\frac{d}{dt} \lambda_i(t) = \kappa \beta_{\lambda_i}^{(1)} + \kappa^2 \beta_{\lambda_i}^{(2)} + \kappa^3 \beta_{\lambda_i}^{(3)} + \dots, \quad (8)$$

where $\kappa = 1/(16\pi^2)$ and the apex on the β -functions represents the loop order. Here, we are interested in the RGE dependence of the couplings ($g, g', g_3, h_t, \lambda, \gamma$). The 1-loop and 2-loop expressions for the β -functions in the SM are well known and can be found *e.g.* in Ford et al. [28]. The complete 3-loop β -functions for the SM have been computed more recently in refs. [29–36]. The dominant 4-loop contribution to the running of the strong gauge coupling has been also computed recently, see refs. [37, 38]. In the present analysis we include all these contributions, as already done in ref. [14].

2.2 RGE-improved effective potential

Without sticking to any specific choice of scale, the RGE-improved effective potential at high field values can be rewritten as

$$V_{\text{eff}}(\phi, t) \approx \frac{\lambda_{\text{eff}}(\phi, t)}{24} \phi^4, \quad (9)$$

where $\lambda_{\text{eff}}(\phi, t)$ takes into account wave function normalization and can be expanded as sum of tree-level plus increasing loop contributions:

$$\lambda_{\text{eff}}(\phi, t) = e^{4\Gamma(t)} \left[\lambda(t) + \lambda^{(1)}(\phi, t) + \lambda^{(2)}(\phi, t) + \dots \right]. \quad (10)$$

In particular, the 1-loop Coleman-Weinberg contribution [39] is

$$\lambda^{(1)}(\phi, t) = 6 \frac{1}{(4\pi)^2} \sum_p N_p \kappa_p^2(t) \left(\log \frac{\kappa_p(t) e^{2\Gamma(t)} \phi^2}{\mu(t)^2} - C_p \right), \quad (11)$$

where, generically, p runs over the contributions of the top quark t , the gauge bosons W and Z , the Higgs boson ϕ and the Goldstone bosons χ . The coefficients N_p , C_p , κ_p are listed in table 1 for the Landau gauge (see *e.g.* table 2 of ref. [40] for a general R_ξ gauge).

p	t	W	Z	ϕ	χ
N_p	-12	6	3	1	3
C_p	3/2	5/6	5/6	3/2	3/2
κ_p	$h^2/2$	$g^2/4$	$(g^2 + g'^2)/4$	3λ	λ

Table 1: Coefficients for eq. (11) in the Landau gauge.

The 2-loop contribution $\lambda^{(2)}(\phi, t)$ was derived by Ford et al. in ref. [28] and, in the limit $\lambda \rightarrow 0$, was cast in a more compact form in refs. [41, 42]. We verified, consistently with these works, that the error committed in this approximation is less than 10% and can thus be neglected.

It is clear that when $\lambda(t)$ becomes negative, the Higgs and Goldstone contributions in eq. (11) are small but complex, and this represents a problem in the numerical analysis of the stability of the electroweak vacuum. Indeed, in refs. [41, 42] the potential was calculated at the 2-loop level, but setting to zero the Higgs and Goldstone contributions in eq. (11). Some authors [43, 44] recently showed that the procedure of refs. [41, 42] is actually theoretically justified when λ is small (say $\lambda \sim \hbar$): in this case, the sum over p does not have to include the Higgs and Goldstone's contributions, which rather have to be accounted for in the 2-loop effective potential, which practically coincides with the expression derived in refs. [41, 42]. For the rising inflection point configuration we are interested in, λ is indeed small: as already done in ref. [14], we thus adopt the procedure outlined in [44]. Explicitly:

$$V_{\text{eff}} = V^{(0)} + V^{(1)} + V^{(2)} + \dots \quad (12)$$

where

$$V^{(0)} = \frac{\lambda(t)}{24} e^{4\Gamma(t)} \phi^4, \quad (13)$$

$$\begin{aligned}
V^{(1)} = & \frac{1}{24} \frac{6}{(4\pi)^2} \left[6 \left(\frac{g(t)^2}{4} \right)^2 \left(\log \frac{\frac{g(t)^2}{4} e^{2\Gamma(t)} \phi^2}{\mu(t)^2} - \frac{5}{6} \right) \right. \\
& + 3 \left(\frac{g(t)^2 + g'(t)^2}{4} \right)^2 \left(\log \frac{\frac{g(t)^2 + g'(t)^2}{4} e^{2\Gamma(t)} \phi^2}{\mu(t)^2} - \frac{5}{6} \right) \\
& \left. - 12 \left(\frac{h(t)^2}{2} \right)^2 \left(\log \frac{\frac{h(t)^2}{2} e^{2\Gamma(t)} \phi^2}{\mu(t)^2} - \frac{3}{2} \right) \right] e^{4\Gamma(t)} \phi^4, \tag{14}
\end{aligned}$$

and $V^{(2)}$ can be found in [41, 42].

A relevant aspect of the present calculation is represented by the well-known fact that the RGE-improved effective potential is gauge dependent. After choosing the renormalization scale t , the RGE-improved effective potential, $V_{\text{eff}}(\phi, \xi)$, is a function of ϕ , the gauge-fixing parameters collectively denoted by ξ , and the other input parameters as m_t , m_H , $\alpha_s^{(5)}$. Due to the explicit presence of ξ in the vacuum stability and/or inflection point conditions, it is not obvious a priori which are the physical (gauge-independent) observables entering the vacuum stability and/or inflection point analysis. The basic tool, in order to capture the gauge-invariant content of the effective potential is given by the Nielsen identity [45]

$$\left(\xi \frac{\partial}{\partial \xi} + C(\phi, \xi) \frac{\partial}{\partial \phi} \right) V_{\text{eff}}(\phi, \xi) = 0, \tag{15}$$

where $C(\phi, \xi)$ is a correlator whose explicit expression will not be needed for our argument. The equation means that $V_{\text{eff}}(\phi, \xi)$ is constant along the characteristics of the equation, which are the curves in the (ϕ, ξ) plane for which $d\xi = \xi/C(\phi, \xi)d\phi$. In particular, the identity says that the effective potential is gauge independent where it is stationary, as happens for two degenerate vacua and for the inflection point configuration. One can also show [14] that the peculiar values of the low energy input parameters (as for instance m_t , the Higgs mass and $\alpha_s^{(5)}$) ensuring stationary configurations are gauge independent.

Working in the Landau gauge is thus perfectly consistent in order to calculate the value of the effective potential at a stationary point, call it V_s , or the value of the input parameters providing it. Nevertheless, one has to be aware that the truncation of the effective potential loop expansion at some loop order, introduces an unavoidable theoretical error both in V_s and in the input parameters. For this sake, it is useful to define the parameter α via

$$\mu(t) = \alpha \phi, \tag{16}$$

and study the dependence of V_s and the input parameters on α . The higher the order of the loop expansion to be considered, the less the dependence on α . This was shown explicitly in [14], where we studied the case of two degenerate vacua and the case of a rising inflection point, respectively; in the following we summarize the main results, as they will be useful also for the analysis of critical Higgs inflation.

2.3 Two degenerate vacua

As discussed in the previous section, once m_H and $\alpha_s^{(5)}$ have been fixed, the value of the top mass for which the SM displays two degenerate vacua, m_t^c , is a gauge invariant quantity. This value

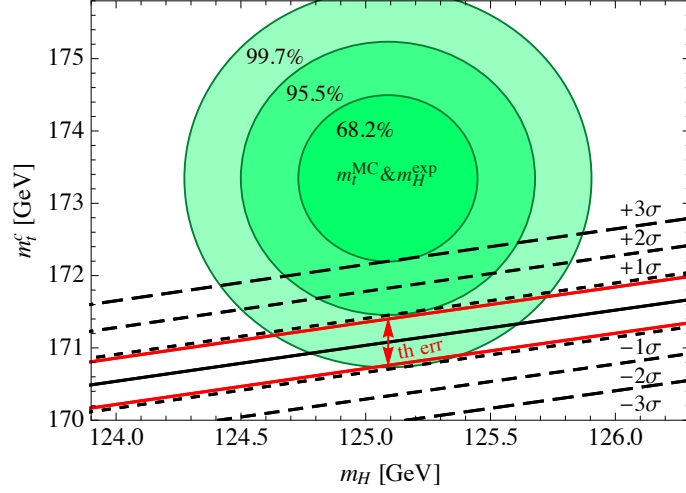


Figure 1: Lines for which the Higgs potential develops a second degenerate minimum at high energy. The solid line corresponds to the central value of $\alpha_s^{(5)}$; the dashed lines are obtained by varying $\alpha_s^{(5)}$ in its experimental range, up to 3σ . The (red) arrow represents the theoretical error in the position of the lines. The (green) shaded regions are the covariance ellipses obtained combining $m_t^{MC} = 173.34 \pm 0.76$ GeV and $m_H^{exp} = 125.09 \pm 0.24$ GeV; the probability of finding m_t^{MC} and m_H inside the inner (central, outer) ellipse is equal to 68.2% (95.5%, 99.7%). The plot is taken from ref. [14].

is however plagued by experimental and theoretical errors. The result of the NNLO calculation is [14]:

$$m_t^c = (171.08 \pm 0.37_{\alpha_s} \pm 0.12_{m_H} \pm 0.32_{th}) \text{ GeV}, \quad (17)$$

where the first two errors are the 1σ variations of $\alpha_s^{(5)}$ and m_H . Our results for the value of m_t^c update and improve but, modulo the doubling of the experimental error in $\alpha_s^{(5)}$, are essentially consistent with those of the literature [21, 41, 42, 46–48].

In fig. 1, m_t^c is displayed as a function of m_H for selected values of $\alpha_s^{(5)}$; in particular, the solid line refers to its central value, while the dotted, short and long dashed lines refer to the 1σ , 2σ and 3σ deviations respectively. In the region below (above) the line the potential is stable (metastable). The theoretical uncertainty on m_t^c due to the NNLO matching turns out to be about ± 0.32 GeV: the position of the straight lines in fig. 1 can be shifted up or down, as represented by the (red) arrow for the central value of $\alpha_s^{(5)}$. The value ± 0.32 GeV is obtained combining in quadrature the error on m_t^c associated to the matching of λ , ± 0.19 GeV for $\pm \Delta\lambda$, and the one associated to the matching of the top Yukawa coupling, ∓ 0.25 GeV for $\pm \Delta y_t$.

The present combined Tevatron and LHC value of the MC top mass is $m_t^{MC} = (173.34 \pm 0.76)$ GeV [24]. Taking into account the theoretical error, we see that the stability line for the central (upper 2σ) value of $\alpha_s^{(5)}$ touches the $m_t^{MC} - m_H^{exp}$ covariance ellipse corresponding to a 95.5% (68.2%) probability. This calculation of the experimental and theoretical uncertainties on m_t^c , in addition to the uncertainty in the identification of the MC and pole top masses, lead us to conclude that stability is at present still compatible with the experimental data at about 2σ [14].

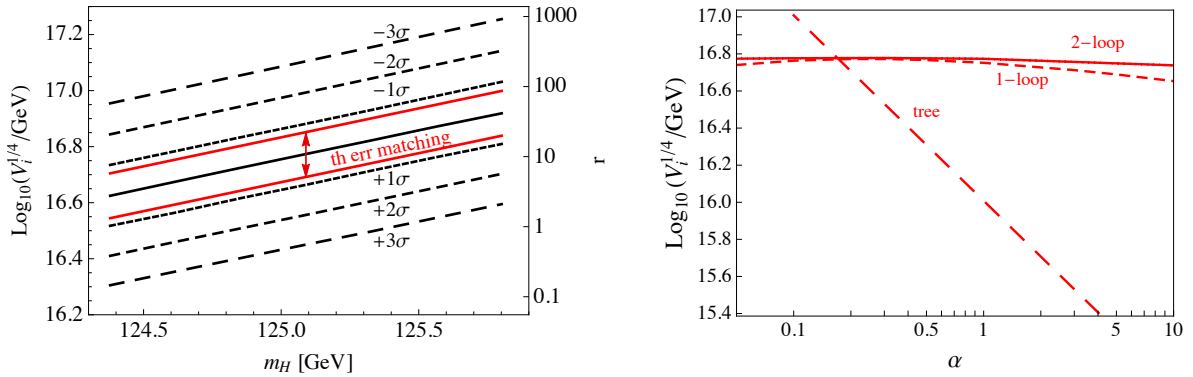


Figure 2: Left: Dependence of $V_i^{1/4}$ on m_H for fixed values of $\alpha_s^{(5)}$. The (red) arrow and solid lines show the theoretical error due to the matching of λ . The right vertical axis displays the associated value of the tensor-to-scalar ratio r , according to eq. (19). Right: Dependence of $V_i^{1/4}$ on α at the tree, 1-loop and 2-loop levels. For definiteness, $\alpha_s^{(5)}$ and m_H are assigned to their central values. The plots are taken from ref. [14].

2.4 Rising inflection point

Such configuration is relevant for the class of models of primordial inflation based on a shallow false minimum [15–18], which was studied in [14], and those based on the non-minimal coupling, which we study in the present work.

The value of the top mass giving the inflection point configuration, m_t^i , is smaller but so close to the one giving two degenerate vacua that eq. (17) applies also in this case.

We denote the value of the Higgs effective potential at the inflection point by V_i . Experimental uncertainties on V_i can be estimated as follows: we let $\alpha_s^{(5)}$ vary in its 3σ experimental range and, for fixed values of m_H , we determine m_t^i and the 2-loop effective potential V_i : the result is displayed in the left panel of fig. 2 (taken from [14]): one can see that increasing $\alpha_s^{(5)}$ from its lower to its upper 3σ range, $V_i^{1/4}$ decreases from 2×10^{17} GeV up to 2×10^{16} GeV; the dependence on m_H is less dramatic.

Theoretical errors can be divided in three categories: those associated to i) the matching, ii) the running, and iii) the effective potential expansion.

i) Theoretical errors associated to the NNLO matching of λ are displayed via the (red) lines in the left panel of fig. 2: the line associated the central value of $\alpha_s^{(5)}$ could be shifted by about ± 0.08 when the quartic coupling changes by $\pm \Delta\lambda$. This theoretical error is thus slightly smaller than the experimental error due to the 1σ variation of $\alpha_s^{(5)}$. The theoretical error in the matching of the top Yukawa coupling has a negligible effect on V_i .

ii) The order of magnitude of the theoretical errors associated to the β -functions at NNLO can be estimated by studying the impact of the subsequent correction; it turns out that such error is negligible.

iii) The theoretical uncertainty associated to the fact that we truncate the effective potential

at some loop level can be estimated by studying the dependence of V_i on α . We fix $\alpha_s^{(5)}$ and m_H at their central values and display in the right panel of fig. 2 the resulting value of $V_i^{1/4}$ at the tree, 1-loop and 2-loops levels by means of the long-dashed, dashed and solid lines respectively. The dependence of $V_i^{1/4}$ on α at the tree-level is implicit, $V_{\text{eff}} \propto \lambda(\ln(\alpha\phi/m_t))$, but significant: it is uncertain by more than one order of magnitude. The 1-loop corrections flattens the dependence on α so that the uncertainty on $V_i^{1/4}$ gets reduced down to about 20%; this uncertainty is comparable to the theoretical one due to the matching. The 2-loop correction further flattens the dependence on α and allows to estimate $V_i^{1/4}$ with a 5% precision.

Summarizing, the result of the NNLO calculation is [14]:

$$\log_{10}(V_i^{1/4}/\text{GeV}) = 16.77 \pm 0.11_{\alpha_s} \pm 0.05_{m_H} \pm 0.08_{th}, \quad (18)$$

where the first two errors refer to the 1σ variations of $\alpha_s^{(5)}$ and m_H respectively, while the theoretical error is dominated by the one in the matching of λ .

2.4.1 Impact on models of inflation with a rising inflection point

A precise determination of V_i is important for models of inflation based on the idea of a shallow false minimum [15–18] as, in these models, V_i and the ratio of the scalar-to-tensor modes of primordial perturbations, r , are linked via:

$$V_i = \frac{3\pi^2}{2} r A_s, \quad (19)$$

where $A_s = 2.2 \times 10^{-9}$ [49] is the amplitude of scalar perturbations. This relation follows from the fact that about 62 e-folds before the end of inflation, the Higgs field (playing the role of a curvaton) is at the inflection point, so that

$$A_s = \frac{H^2}{8\pi^2\epsilon} \Big|_{N=62}, \quad (20)$$

where $H^2 \approx V_i/3$ is the Hubble parameter (dominated by the SM potential), and the inflaton is in a slow-roll phase, so that $r = 16\epsilon$.

In view of such application, the right axis of the plot in the left panel of fig. 2 reports the corresponding value of r . The dependence of r on $\alpha_s^{(5)}$ is strong: when the latter is varied in its 3σ range, r spans about three orders of magnitude, from 0.3 to 300. The dependence on m_H is milder. The theoretical error in the matching of λ implies an uncertainty on r by a factor of about 2.

According to the 2015 analysis of the Planck Collaboration, the present upper bound on r at the pivot scale $k_* = 0.002 \text{ Mpc}^{-1}$ is $r < 0.12$ at 95% C.L. [12], as also confirmed by the recent joint analysis with the BICEP2 Collaboration [13]. Due to eq. (19), this would translate into the 95% C.L. bound

$$\log_{10}(V_i^{1/4}/\text{GeV}) < 16.28, \quad (21)$$

which implies a tension with eq. (18) at about 4σ with respect to $\alpha_s^{(5)}$. This tension might be reduced at about 3σ assuming the theoretical error on the matching of λ to go in the "right" direction of lowering V_i (this would correspond to $+\Delta\lambda$, which however goes in the "wrong"

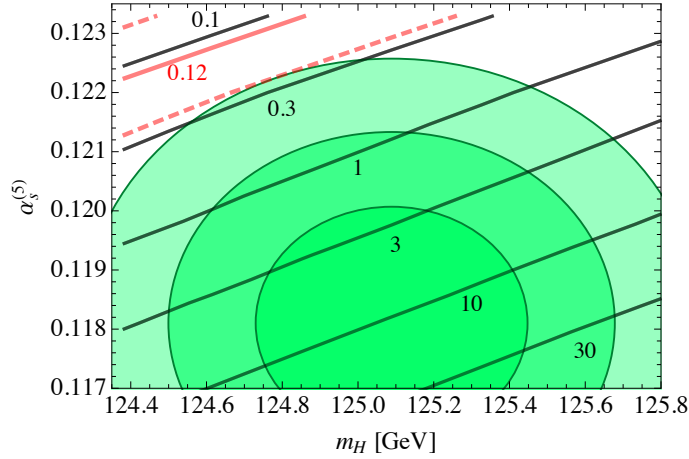


Figure 3: Contour levels of r in the plane $(m_H, \alpha_s^{(5)})$. The theoretical uncertainty corresponding to $r = 0.12$ is shown by means of the (red) dashed lines. The shaded regions are the covariance ellipses indicating that the probability of finding the experimental values of m_H and $\alpha_s^{(5)}$ inside the ellipses are respectively 68.2%, 95.4%, 99.7%. The plot is taken from ref. [14].

direction for the sake of m_t^c). This can be graphically seen in fig. 3, where the contour levels of r in the plane $(m_H, \alpha_s^{(5)})$ are shown. Even invoking the uncertainty due to the matching (lower red-dashed lines), a value for r as small as 0.12 (red-solid line), could be obtained only with $\alpha_s^{(5)}$ to take its upper 3σ value, and m_H its lower 1σ one; the value of m_t could stay around its lower 1.5σ value, as can be see from fig. 1.

These considerations will be useful also for the model of critical Higgs inflation, which however requires a specific study. In the next section we review this model, paying attention to work at least at 1-loop in the expansion of the effective potential.

3 Higgs Inflation: the model

We introduce a non-minimal gravitational coupling ξ between the SM Higgs doublet \mathcal{H} and the Ricci scalar R [7]:

$$\mathcal{S} = \int d^4x \sqrt{-g} \left[\mathcal{L}_{SM} - \frac{M_P^2}{2} R - \xi |\mathcal{H}|^2 R \right], \quad (22)$$

where \mathcal{L}_{SM} is the Standard Model Lagrangian, $M_P = 1/(8\pi G_N)^{1/2} \simeq 2.43 \times 10^{18}$ GeV is the reduced Planck mass and g is the determinant of the Friedmann-Lemâitre-Robertson-Walker metric. The relevant part of the action (22) from a cosmological point of view is:

$$\mathcal{S}_J = \int d^4x \sqrt{-g} \left[|\partial \mathcal{H}|^2 - \frac{M_P^2}{2} R - \xi |\mathcal{H}|^2 R - V \right], \quad (23)$$

where V is the SM potential of eq. (1), $|\partial \mathcal{H}|^2 = (\partial_\mu \mathcal{H})^\dagger (\partial^\mu \mathcal{H})$ and the subscript J means that the action is evaluated in the Jordan frame (where physical distances are measured and the

inflationary model is defined). In order to remove the non-minimal coupling we introduce a conformal (or Weyl) transformation:

$$g_{\mu\nu} \rightarrow \tilde{g}_{\mu\nu} = \Omega^{-2} g_{\mu\nu}, \quad \Omega^2 \equiv 1 + 2\xi \frac{|\mathcal{H}|^2}{M_P^2}. \quad (24)$$

If we further consider the unitary gauge, in which the only scalar field is the radial mode $\phi = \sqrt{2|\mathcal{H}|^2}$, we obtain the Einstein frame action where gravity is canonically normalized:

$$\mathcal{S}_E = \int d^4x \sqrt{-\tilde{g}} \left[-\frac{M_P^2}{2} \tilde{R} + K \frac{(\partial\phi)^2}{2} - \frac{V}{\Omega^4} \right], \quad K = \frac{\Omega^2 + \frac{3}{2} \left(\frac{d\Omega^2}{d\phi} \right)^2}{\Omega^4}. \quad (25)$$

The kinetic term for the Higgs field in (25) can be made canonical by the redefinition $\phi = \phi(\chi)$:

$$\frac{d\chi}{d\phi} = \sqrt{\frac{\Omega^2 + \frac{3}{2} \left(\frac{d\Omega^2}{d\phi} \right)^2}{\Omega^4}}, \quad \phi(\chi = 0) = 0. \quad (26)$$

From now on the bar over a quantity will indicate that it is given in (reduced) Planck units. Since $\phi(\chi)$ is invertible, one can obtain a closed analytical relation between the two fields:

$$\bar{\chi}(\bar{\phi}) = \sqrt{\frac{1+6\xi}{\xi}} \sinh^{-1} \left(\sqrt{\xi(1+6\xi)} \bar{\phi} \right) - \sqrt{6} \tanh^{-1} \left(\frac{\sqrt{6\xi} \bar{\phi}}{\sqrt{1+\xi(1+6\xi)} \bar{\phi}^2} \right). \quad (27)$$

The final expression for the Einstein frame action is

$$\mathcal{S}_E = \int d^4x \sqrt{-\tilde{g}} \left[-\frac{M_P^2}{2} \tilde{R} + \frac{(\partial\chi)^2}{2} - U \right], \quad (28)$$

where the potential U felt by χ is

$$U = \frac{V}{\Omega^4}. \quad (29)$$

Hence, at tree-level

$$U = \frac{\lambda}{24} \frac{(\phi(\chi)^2 - v^2)^2}{(1 + \xi \bar{\phi}(\chi)^2)^2} \simeq \frac{\lambda}{24} \frac{\phi(\chi)^4}{(1 + \xi \bar{\phi}(\chi)^2)^2}. \quad (30)$$

The potential is exponentially flat for large field values and can in principle provide a slow-roll inflationary phase.

3.1 Radiative corrections

We turn to consider the inclusion of radiative corrections: the running of the couplings, now including also the running of the non-minimal coupling ξ , see e.g. [50], and the loop corrections to the effective potential.

The non-minimal coupling ξ affects the running through the appearance of a factor s that suppresses the contribution of the physical Higgs to the RGEs [50, 51]:

$$s(\phi) = \frac{1 + \xi \bar{\phi}^2}{1 + (1 + 6\xi) \xi \bar{\phi}^2}. \quad (31)$$

For small field values $\bar{\phi} \ll 1/\sqrt{\xi}$, $s \simeq 1$, recovering the SM case; in the inflationary regime $\bar{\phi} \gg 1/\sqrt{\xi}$, the RG equations differ from those of the SM as quantum loops involving the Higgs field are heavily suppressed.

The total RG-improved effective potential is given by

$$U_{\text{eff}} = U^{(0)} + U^{(1)} + U^{(2)} + \dots, \quad (32)$$

with the running of all the couplings involved, evaluated at some renormalization scale $\mu(t)$, conveniently chosen in order to minimize the effect of the logarithms.

There exist two options for the quantization of the classical theory - see e.g. [50, 52] for recent reviews. One can compute quantum corrections to the potential after the transformation (24), in the Einstein frame (prescription I) [7] or before, directly in the Jordan frame (prescription II) [53].

According to prescription I, the tree-level SM potential is first rewritten in the Einstein frame giving

$$U^{(0)} = \frac{\lambda(t)}{24} \frac{e^{4\Gamma(t)} \phi^4}{\Omega^4}, \quad \Omega^2 = 1 + \xi(t) e^{2\Gamma(t)} \bar{\phi}^2, \quad (33)$$

where $\Gamma(t)$ takes into account the wave function renormalization of ϕ . The 1-loop corrections take the form of (14), but the particle masses are computed from the tree-level potential above: this means that the quantity κ_p of table 1 displays a suppression factor Ω^2 for the W, Z, t contributions (while the Higgs and Goldstone contribution belong to $U^{(2)}$):

$$\begin{aligned} U^{(1)} = & \frac{1}{24} \frac{6}{(4\pi)^2} \left[6 \left(\frac{g(t)^2}{4} \right)^2 \left(\log \frac{\frac{g(t)^2}{4} e^{2\Gamma(t)} \phi^2}{\mu(t)^2 \Omega^2} - \frac{5}{6} \right) \right. \\ & + 3 \left(\frac{g(t)^2 + g'(t)^2}{4} \right)^2 \left(\log \frac{\frac{g(t)^2 + g'(t)^2}{4} e^{2\Gamma(t)} \phi^2}{\mu(t)^2 \Omega^2} - \frac{5}{6} \right) \\ & \left. - 12 \left(\frac{h(t)^2}{2} \right)^2 \left(\log \frac{\frac{h(t)^2}{2} e^{2\Gamma(t)} \phi^2}{\mu(t)^2 \Omega^2} - \frac{3}{2} \right) \right] \frac{e^{4\Gamma(t)} \phi^4}{\Omega^4}. \end{aligned} \quad (34)$$

The 2-loop radiative corrections $U^{(2)}$ can be found in the same way, operating on the explicit form given in [41, 42]. The appropriate scale for minimizing the effect of the logarithms is given by ϕ/Ω . As done in the previous section, we define the parameter α via

$$\mu(t) = \alpha \frac{\phi}{\Omega}. \quad (35)$$

According to prescription II, the radiative corrections are evaluated directly in the Jordan frame, before the conformal transformation: they are thus given by $V^{(1)}$ of eq. (14). After going in the Einstein frame, the tree-level potential is thus the same as (33), while $U^{(1)} = V^{(1)}/\Omega^4$

becomes

$$\begin{aligned}
U^{(1)} = & \frac{1}{24} \frac{6}{(4\pi)^2} \left[6 \left(\frac{g(t)^2}{4} \right)^2 \left(\log \frac{\frac{g(t)^2}{4} e^{2\Gamma(t)} \phi^2}{\mu(t)^2} - \frac{5}{6} \right) \right. \\
& + 3 \left(\frac{g(t)^2 + g'(t)^2}{4} \right)^2 \left(\log \frac{\frac{g(t)^2 + g'(t)^2}{4} e^{2\Gamma(t)} \phi^2}{\mu(t)^2} - \frac{5}{6} \right) \\
& \left. - 12 \left(\frac{h(t)^2}{2} \right)^2 \left(\log \frac{\frac{h(t)^2}{2} e^{2\Gamma(t)} \phi^2}{\mu(t)^2} - \frac{3}{2} \right) \right] \frac{e^{4\Gamma(t)} \phi^4}{\Omega^4}.
\end{aligned} \tag{36}$$

Now it make sense to define the parameter α as in eq. (16), namely

$$\mu(t) = \alpha \phi. \tag{37}$$

We can recognize that, due to the different choices of $\mu(t)$, the two prescriptions are formally equivalent up to 1-loop. This is due to the fact that for λ small, the contribution of the Higgs and would de Goldstone bosons have to be included in the 2-loop contribution.

So, in practice, the difference between the effective potentials for the two renormalization prescriptions is the functional dependence $t = t(\phi)$. For prescription I, $t = \ln[(\alpha\phi)/(\Omega m_t)]$ approaches a constant value in the inflationary region $\phi \gtrsim M_{Pl}/\sqrt{\xi}$, and hence so do the couplings $g(t), g'(t)$, etc. For prescription II, $t = \ln[(\alpha\phi)/m_t]$ does not approach a constant value. As a result, the effective potential for prescription I approaches a constant value in the inflationary region (even after including radiative corrections) while the effective potential for prescription II, due to the continued running of the couplings, does not.

This difference can have an impact on Higgs inflation and its predictions. In the case of critical Higgs inflation, however, there is no difference as far as we analyze the potential close to the inflection point (where $\Omega \approx 1$), as will be shown in the following. From now on, we will follow prescription I for definiteness.

Before proceeding, it is important to understand the size of the theoretical error associated to the truncation of the effective potential at a certain loop order. This error can be estimated by varying α , as done in the previous section. However, now that we apply this method to the model with the non-minimal coupling, we have also to take into account the effect of ξ . As far as ξ is small, the plateau induced by it starts at higher field values than those of the inflection point, so that $U_i \approx V_i$. We can thus recover the results of fig. 2 (right panel), where we see that the better choice to reduce the logarithm is to take α in the range 0.1 – 1: the tree-level potential displays a large variation with α , but the 1-loop effective potential is reliable enough, in particular for the value $\alpha = 0.3$, where it coincides with the 2-loop effective potential.

To see directly this, in the upper panel of fig. 4, we display the tree level potential $U^{(0)}$ as a function of $\bar{\phi}$, taking $\alpha = 0.1, 0.3, 1$, in the left, middle and right panel respectively. From top (solid) to bottom (long-dashed) the lines correspond to $\xi = 0, 0.1, 1, 10$. The central values are taken for $\alpha_s^{(5)}$ and m_H . We can see that the highness of the inflection point is uncertain by one order of magnitude. The value of ϕ where the inflection point occurs (a quantity that is not gauge invariant) is also quite undetermined: the same value of ξ (e.g. $\xi = 10$) gives rise to a potential with an inflection point before the plateau for $\alpha = 1$, while for $\alpha = 0.1$ the plateau

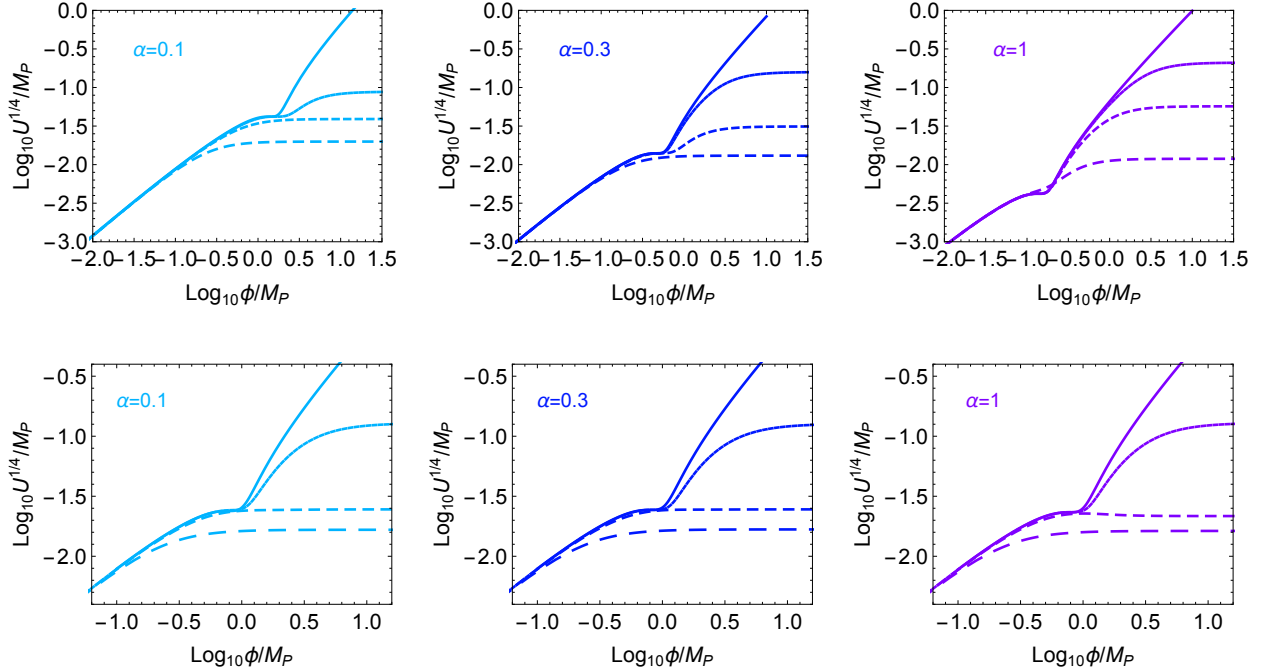


Figure 4: The RGE-improved potential U is shown as a function of ϕ for $\alpha = 0.1, 0.3, 1$, in the left, middle and right panel respectively. From top (solid) to bottom (long-dashed) the lines correspond to $\xi = 0, 0.1, 1, 10$. Central values taken for $\alpha_s^{(5)}$ and m_H . Upper panel: tree-level calculation. Lower panel: 1-loop calculation.

starts before the inflection point. This simply means that the tree-level potential, even improved with matching and running at NNLO, is not reliable.

In the lower panel of fig. 4 we display the effective potential U_{eff} at 1-loop as a function of $\bar{\phi}$, taking $\alpha = 0.1, 0.3, 1$. We can see that these plots are essentially undistinguishable. This means that the 1-loop effective potential is trustable for the sake of the present analysis. In the following, we will thus consider the effective potential expansion at 1-loop, with $\alpha = 0.3$ (for which the result of the 2-loop effective potential expansion is reproduced): in this way, the theoretical error associated to the truncation of the effective potential is smaller than the theoretical error associated to the matching of λ .

4 The inflection point of Critical Higgs inflation

We are now in the position to study in detail the potential corresponding to a critical configuration, first in terms of ϕ and then expressing the potential as a function of χ , which is necessary to study the dynamics of inflation.

The critical configuration is achieved when there is an inflection point at some field value ϕ_i ,

and the plateau induced by the non-minimal coupling ξ starts at a value $\phi_\xi > \phi_i$. The inflection point is at a value of ϕ_i which is fixed by the experimental window of the input parameters, namely $\alpha_s^{(5)}$ and m_H (m_t is chosen accordingly), while the plateau starts at $\bar{\phi}_\xi \approx 1/\sqrt{\xi}$.

The bottom central panel of fig. 4 shows that, taking $\alpha_s^{(5)}$ and m_H at their central values, $\bar{\phi}_i \approx 1$ and $\bar{U}_i^{1/4} \approx 10^{-1.6}$ (namely $U_i^{1/4} \approx 6 \times 10^{16}$ GeV). The value of ϕ_i is not gauge invariant, but the highness of the potential at the inflection point, \bar{U}_i , is (see the discussion in the previous chapter). Only with $\xi \lesssim 1$ one can have a critical configuration: with larger values the plateau destroys the inflection point.

Notice that, in a critical configuration, as far as we consider field values close to ϕ_i , we have $\Omega \approx 1$. This has two implications. Firstly, $U_i \approx V_i$ and we can apply here too all the discussion made in section 2.4. Secondly, the relation between the renormalization parameter t and ϕ is the same for the two prescriptions, see eqs. (35) and (37): the value of U_i is thus not plagued by the issue of the prescription (the behavior at the plateau actually is, but this will turn out to be not relevant for the sake of our discussion).

The small value of ξ required for critical inflation is particularly interesting, as it is related to one of the most significant drawbacks of Higgs inflation: the violation of perturbative unitarity at the scale $\bar{\phi}_U \approx 1/\xi$. For $\xi < 1$ this scale is pushed at higher values than the inflationary scale $\bar{\phi}_\xi$ and the questionable assumptions of non-renormalizable operators or new strong dynamics entering to restore unitarity are no longer required (see e.g. [50] and references therein).

We now turn to the field χ , which allows to better inspect the dynamics of inflation. In the left panel of fig. 5 we reproduce the same configuration shown in the bottom central panel of fig. 4, obtained taking $\alpha_s^{(5)}$ and m_H at their central values and $m_t = 171.08$ GeV. Clearly, the value of the effective potential at the inflection point does not change upon this substitution, as the relation between ϕ and χ is a monotonically increasing one. We see again that criticality, namely $\bar{\chi}_\xi > \bar{\chi}_i$, requires $\xi \lesssim 1$.

Once the shape of $U(\chi)$ is known, it is possible to calculate the inflationary observables. The equation of motion of the field $\chi(t)$ is

$$\chi(t)'' + 3H(t)\chi(t) = -\frac{dU}{d\chi}(\chi(t)) \ , \ H(t)^2 = \frac{1}{3} \left(U(\chi(t)) + \frac{1}{2}\chi(t)^2 \right) \ , \quad (38)$$

where the initial conditions are $\chi(t_0) = \chi_0$, $\chi'(t_0) = \chi'_0$, and t_0 is some initial time. The time duration of the inflationary phase is represented by the number of e-folds,

$$N = \int_{t_b}^{t_e} dt H(t) \ , \quad (39)$$

where t_e is the time of the end of inflation and $t_b > t_0$ is the time when the inflationary CMB observables, like A_s, n_s, r , are measured. It is known that t_b is such that $N \approx 62$.

The critical configuration has received interest in relation to the generation of primordial black holes [1]. The idea is that the field χ is slowly rolling on top of the non-minimal plateau about 62 e-folds before the end of inflation: CMB observables are measured at that epoch. Initial conditions are not even relevant [11]. About 20 – 30 e-folds before the end of inflation, the field χ crosses the inflection point where it slows considerably: this gives rise to a peak in the power spectrum of primordial curvature perturbations, which also results in a peculiar phenomenology for black holes, enhancing those that could significantly contribute to dark matter today [1–3].

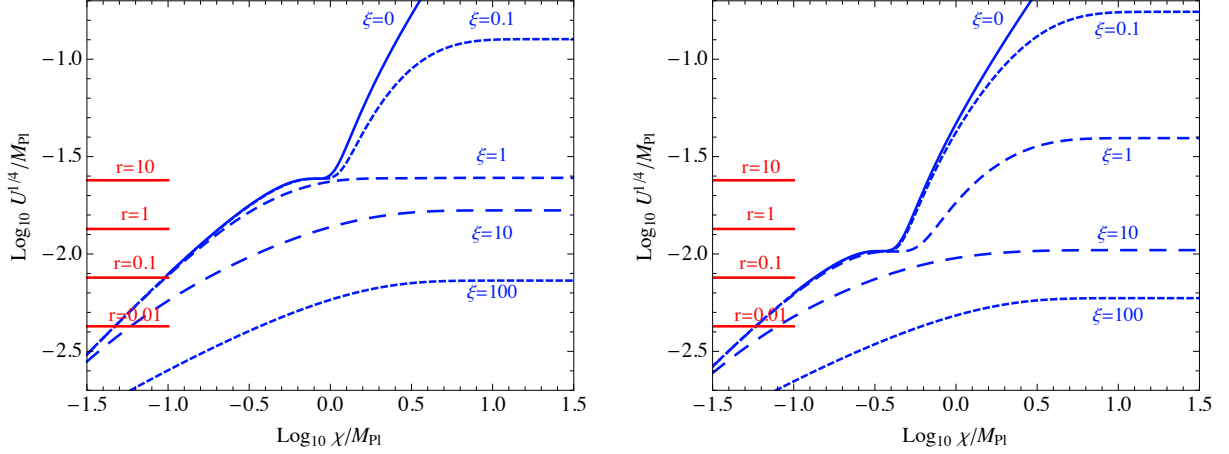


Figure 5: The potential U is shown as a function of χ (for $\alpha = 0.3$). From top (solid) to bottom (long-dashed) the lines correspond to $\xi = 0, 0.1, 1, 10, 100$. Left: Central values taken for $\alpha_s^{(5)}$ and $m_H, m_t = 171.08$ GeV. Right: $\alpha_s^{(5)}$ is at its 3σ upper value, m_H at its lower 1σ , $m_t = 172.08$ GeV.

In a critical configuration, the Hubble constant at the non-minimal plateau is higher than at the inflection point. Similarly to the discussion in the previous section, we can derive an upper bound on U_i from the experimental upper bound on the tensor-to-scalar ratio r :

$$A_s = \frac{H^2}{8\pi^2\epsilon} \big|_{N=62} \simeq \frac{U}{24\pi^2\epsilon} \big|_{N=62} \simeq \frac{2U|_{N=62}}{3\pi^2 r} \gtrsim \frac{2U_i}{3\pi^2 r}, \quad (40)$$

where the last inequality holds because $U|_{N=62} \gtrsim U_i$. We thus have

$$U_i \lesssim \frac{3\pi^2}{2} r A_s. \quad (41)$$

Since $U_i \approx V_i$ in a critical configuration, we can apply all the discussion made in section 2.4 for the inflection point of the SM.

So, without any further calculation, just looking at fig. 3, we can conclude that, for the present central values of $\alpha_s^{(5)}$ and m_H , critical Higgs inflation would predict $r \sim 10$; the dominant theoretical error in the calculation is the one associated to the matching of λ and amounts to a factor of about 2. Even assuming that the theoretical error goes in the "right" direction of lowering r , in order to fulfill the present upper bound $r < 0.12$ [12, 13], $\alpha_s^{(5)}$ should be set at its upper 3σ value and m_H at its lower 1σ one.

We can see directly this tension looking at fig. 5, where the red horizontal segments show the values of r according to the relation $r = 2U/(3\pi^2 A_s)$. The plot in the left panel shows that, for the central values of $\alpha_s^{(5)}$ and m_H , the critical configuration predicts $r \gtrsim 10$. The present bound on r implies that Higgs inflation is allowed only with $\xi \gtrsim 100$, hence far from criticality.

In the right panel of fig. 5 we take $\alpha_s^{(5)}$ at its 3σ upper value and m_H at its lower 1σ value: now we see that critical Higgs inflation would predict $r \gtrsim 0.3$. It would be possible to reduce the prediction down to $r \sim 0.12$ only invoking the theoretical error, and taking a suitable value

for ξ . If one does not, the present bound on r implies that Higgs inflation is allowed only with $\xi \gtrsim 10$, far from criticality.

Measuring r close to its present upper bound would thus be compatible with Higgs inflation, but not in its critical version. This would reasonably imply that the production of black holes during inflation is insufficient to constitute a significant fraction of the dark matter seen today.

5 Discussion and conclusions

We studied carefully the model of critical Higgs inflation [4–6], calculating the Higgs effective potential according to the present state of the art, that is the NNLO. We found that, in order to satisfy the present upper bound on the tensor-to-scalar-ratio, $r < 0.12$ [12, 13], while accounting for the correct amplitude of scalar perturbations, one should take $\alpha_s^{(5)}$ at its upper 4σ value, namely $\alpha_s^{(5)} = 0.1233$. This tension can be alleviated at 3σ by invoking the theoretical error (the dominant one is associated to the matching of λ) to go in the right direction.

Is $\alpha_s^{(5)} = 0.1233$ too large? The current 1σ world average, $\alpha_s^{(5)} = 0.1181 \pm 0.0013$ [22], is the result of a fit of many measurements: those pointing to small values are the ones related to structure functions; lattice results also point towards small values, especially because the precision should be better than for other measurements; electroweak precision fits provide a larger error, so that $\alpha_s^{(5)} = 0.1196 \pm 0.0030$. Anyway, looking at fig. 9.2 of the PDG review on Quantum Chromodynamics [22], it seems quite unrealistic that $\alpha_s^{(5)}$ will turn out to be at the level of 0.1233.

Assuming that the present 1σ world average of $\alpha_s^{(5)}$ will be confirmed in the future, one has to conclude that the model of critical Higgs inflation is in serious trouble *per se*, as it badly violates the present bound $r < 0.12$ [12, 13]. A fortiori, it is quite unrealistic that it might account for a significant fraction of the dark matter seen today under the form of primordial black holes.

Unless $\alpha_s^{(5)}$ will turn out to be significantly larger than now estimated, two options are left: 1) Higgs inflation [7, 8] is indeed the right model of primordial inflation, but it is realized in a non-critical form. Primordial black holes might be generated, but it is likely that they marginally contribute to the dark matter seen today; 2) the shape of the inflationary potential is indeed similar to the one of critical Higgs inflation, but V_i is significantly lowered because of the effects of new physics. In principle, in this case primordial black holes might contribute to the dark matter [2, 3]. We checked that right-handed neutrinos would not help (as they have the same effect of enhancing the value of m_t). Maybe it would be more promising to introduce another scalar, but then the model would no more be of single field inflation, and the analysis would be accordingly more complicated.

Acknowledgements

We thanks the CERN Theory Department for kind hospitality and support during the completion of this work. We acknowledge partial support by the research project TAsP (Theoretical Astroparticle Physics) funded by the Istituto Nazionale di Fisica Nucleare (INFN).

References

- [1] J. M. Ezquiaga, J. Garcia-Bellido, E. Ruiz Morales, Primordial Black Hole production in Critical Higgs Inflation, *Phys. Lett. B* 776 (2018) 345–349. [arXiv:1705.04861](#), [doi:10.1016/j.physletb.2017.11.039](#).
- [2] J. Garcia-Bellido, Massive Primordial Black Holes as Dark Matter and their detection with Gravitational Waves, *J. Phys. Conf. Ser.* 840 (1) (2017) 012032. [arXiv:1702.08275](#), [doi:10.1088/1742-6596/840/1/012032](#).
- [3] G. Ballesteros, M. Taoso, Primordial black hole dark matter from single field inflation, *Phys. Rev. D* 97 (2) (2018) 023501. [arXiv:1709.05565](#), [doi:10.1103/PhysRevD.97.023501](#).
- [4] F. Bezrukov, M. Shaposhnikov, Higgs inflation at the critical point. [arXiv:1403.6078](#).
- [5] Y. Hamada, H. Kawai, K.-y. Oda, S. C. Park, Higgs Inflation is Still Alive after the Results from BICEP2, *Phys. Rev. Lett.* 112 (24) (2014) 241301. [arXiv:1403.5043](#), [doi:10.1103/PhysRevLett.112.241301](#).
- [6] Y. Hamada, H. Kawai, K.-y. Oda, S. C. Park, Higgs inflation from Standard Model criticality, *Phys. Rev. D* 91 (2015) 053008. [arXiv:1408.4864](#), [doi:10.1103/PhysRevD.91.053008](#).
- [7] F. Bezrukov, M. Shaposhnikov, The Standard Model Higgs boson as the inflaton, *Phys. Lett. B* 659 (2008) 703–706. [arXiv:0710.3755](#), [doi:10.1016/j.physletb.2007.11.072](#).
- [8] F. Bezrukov, M. Shaposhnikov, Standard Model Higgs boson mass from inflation: Two loop analysis, *JHEP* 0907 (2009) 089. [arXiv:0904.1537](#), [doi:10.1088/1126-6708/2009/07/089](#).
- [9] P. Ade, et al., Detection of B-Mode Polarization at Degree Angular Scales by BICEP2, *Phys. Rev. Lett.* 112 (2014) 241–101. [arXiv:1403.3985](#), [doi:10.1103/PhysRevLett.112.241101](#).
- [10] F. Bezrukov, A. Magnin, M. Shaposhnikov, S. Sibiryakov, Higgs inflation: consistency and generalisations, *JHEP* 01 (2011) 016. [arXiv:1008.5157](#), [doi:10.1007/JHEP01\(2011\)016](#).
- [11] A. Salvio, Initial Conditions for Critical Higgs Inflation, *Phys. Lett. B* 780 (2018) 111–117. [arXiv:1712.04477](#), [doi:10.1016/j.physletb.2018.03.009](#).
- [12] P. A. R. Ade, et al., Planck 2015 results. XX. Constraints on inflation. [arXiv:1502.02114](#).
- [13] P. Ade, et al., Joint Analysis of BICEP2/*Keck Array* and *Planck* Data, *Phys. Rev. Lett.* 114 (2015) 101301. [arXiv:1502.00612](#), [doi:10.1103/PhysRevLett.114.101301](#).
- [14] G. Iacobellis, I. Masina, Stationary configurations of the Standard Model Higgs potential: electroweak stability and rising inflection point, *Phys. Rev. D* 94 (7) (2016) 073005. [arXiv:1604.06046](#), [doi:10.1103/PhysRevD.94.073005](#).
- [15] I. Masina, A. Notari, The Higgs mass range from Standard Model false vacuum Inflation in scalar-tensor gravity, *Phys. Rev. D* 85 (2012) 123506. [arXiv:1112.2659](#), [doi:10.1103/PhysRevD.85.123506](#).

- [16] I. Masina, A. Notari, Standard Model False Vacuum Inflation: Correlating the Tensor-to-Scalar Ratio to the Top Quark and Higgs Boson masses, *Phys.Rev.Lett.* 108 (2012) 191302. [arXiv:1112.5430](#), [doi:10.1103/PhysRevLett.108.191302](#).
- [17] I. Masina, A. Notari, Inflation from the Higgs field false vacuum with hybrid potential, *JCAP* 1211 (2012) 031. [arXiv:1204.4155](#), [doi:10.1088/1475-7516/2012/11/031](#).
- [18] I. Masina, The Gravitational Wave Background and Higgs False Vacuum Inflation, *Phys.Rev. D* 89 (2014) 123505. [arXiv:1403.5244](#), [doi:10.1103/PhysRevD.89.123505](#).
- [19] K. A. Olive, et al., Review of Particle Physics, *Chin. Phys.* C38 (2014) 090001. [doi:10.1088/1674-1137/38/9/090001](#).
- [20] S. Coleman, E. Weinberg, Radiative Corrections as the Origin of Spontaneous Symmetry Breaking, *Phys. Rev. D* 7 (1973) 1888–1910. [doi:10.1103/PhysRevD.7.1888](#).
- [21] A. V. Bednyakov, B. A. Kniehl, A. F. Pikelner, O. L. Veretin, Stability of the Electroweak Vacuum: Gauge Independence and Advanced Precision, *Phys. Rev. Lett.* 115 (20) (2015) 201802. [arXiv:1507.08833](#), [doi:10.1103/PhysRevLett.115.201802](#).
- [22] C. Patrignani, et al., Review of Particle Physics, *Chin. Phys.* C40 (10) (2016) 100001. [doi:10.1088/1674-1137/40/10/100001](#).
- [23] G. Aad, et al., Combined Measurement of the Higgs Boson Mass in pp Collisions at $\sqrt{s} = 7$ and 8 TeV with the ATLAS and CMS Experiments, *Phys. Rev. Lett.* 114 (2015) 191803. [arXiv:1503.07589](#), [doi:10.1103/PhysRevLett.114.191803](#).
- [24] G. Aad, et al., First combination of Tevatron and LHC measurements of the top-quark mass. [arXiv:1403.4427](#).
- [25] P. Nason, Theory Summary. [arXiv:1602.00443](#).
- [26] G. Corcella, Interpretation of the top-quark mass measurements: a theory overview, in: 8th International Workshop on Top Quark Physics (TOP2015) Ischia, NA, Italy, September 14-18, 2015, 2015. [arXiv:1511.08429](#).
- [27] S. Moch, et al., High precision fundamental constants at the TeV scale. [arXiv:1405.4781](#).
- [28] C. Ford, I. Jack, D. R. T. Jones, The Standard model effective potential at two loops, *Nucl. Phys. B* 387 (1992) 373–390, [Erratum: *Nucl. Phys.* B504,551(1997)]. [arXiv:hep-ph/0111190](#), [doi:10.1016/0550-3213\(92\)90165-8](#).
- [29] L. N. Mihaila, J. Salomon, M. Steinhauser, Gauge Coupling β -functions in the Standard Model to Three Loops, *Phys. Rev. Lett.* 108 (2012) 151602. [arXiv:1201.5868](#), [doi:10.1103/PhysRevLett.108.151602](#).
- [30] L. N. Mihaila, J. Salomon, M. Steinhauser, Renormalization constants and β -functions for the gauge couplings of the Standard Model to three-loop order, *Phys. Rev. D* 86 (2012) 096008. [arXiv:1208.3357](#), [doi:10.1103/PhysRevD.86.096008](#).

- [31] K. G. Chetyrkin, M. F. Zoller, Three-loop β -functions for top-Yukawa and the Higgs self-interaction in the Standard Model, JHEP 06 (2012) 033. [arXiv:1205.2892](#), [doi:10.1007/JHEP06\(2012\)033](#).
- [32] K. G. Chetyrkin, M. F. Zoller, β -function for the Higgs self-interaction in the Standard Model at three-loop level, JHEP 04 (2013) 091, [Erratum: JHEP09,155(2013)]. [arXiv:1303.2890](#), [doi:10.1007/JHEP04\(2013\)091](#), [doi:10.1007/JHEP09\(2013\)155](#).
- [33] A. V. Bednyakov, A. F. Pikelner, V. N. Velizhanin, Higgs self-coupling β -function in the Standard Model at three loops, Nucl. Phys. B875 (2013) 552–565. [arXiv:1303.4364](#), [doi:10.1016/j.nuclphysb.2013.07.015](#).
- [34] A. V. Bednyakov, A. F. Pikelner, V. N. Velizhanin, Yukawa coupling β -functions in the Standard Model at three loops, Phys. Lett. B722 (2013) 336–340. [arXiv:1212.6829](#), [doi:10.1016/j.physletb.2013.04.038](#).
- [35] A. V. Bednyakov, A. F. Pikelner, V. N. Velizhanin, Three-loop Higgs self-coupling β -function in the Standard Model with complex Yukawa matrices, Nucl. Phys. B879 (2014) 256–267. [arXiv:1310.3806](#), [doi:10.1016/j.nuclphysb.2013.12.012](#).
- [36] A. V. Bednyakov, A. F. Pikelner, V. N. Velizhanin, Three-loop SM β -functions for matrix Yukawa couplings, Phys. Lett. B737 (2014) 129–134. [arXiv:1406.7171](#), [doi:10.1016/j.physletb.2014.08.049](#).
- [37] M. F. Zoller, Top-Yukawa effects on the β -function of the strong coupling in the SM at four-loop level, JHEP 02 (2016) 095. [arXiv:1508.03624](#), [doi:10.1007/JHEP02\(2016\)095](#).
- [38] A. V. Bednyakov, A. F. Pikelner, Four-loop strong coupling β -function in the Standard Model. [arXiv:1508.02680](#).
- [39] S. R. Coleman, E. J. Weinberg, Radiative Corrections as the Origin of Spontaneous Symmetry Breaking, Phys. Rev. D7 (1973) 1888–1910. [doi:10.1103/PhysRevD.7.1888](#).
- [40] L. Di Luzio, L. Mihaila, On the gauge dependence of the Standard Model vacuum instability scale, JHEP 06 (2014) 079. [arXiv:1404.7450](#), [doi:10.1007/JHEP06\(2014\)079](#).
- [41] G. Degrandi, S. Di Vita, J. Elias-Miro, J. R. Espinosa, G. F. Giudice, et al., Higgs mass and vacuum stability in the Standard Model at NNLO, JHEP 1208 (2012) 098. [arXiv:1205.6497](#), [doi:10.1007/JHEP08\(2012\)098](#).
- [42] D. Buttazzo, G. Degrandi, P. P. Giardino, G. F. Giudice, F. Sala, A. Salvio, A. Strumia, Investigating the near-criticality of the Higgs boson, JHEP 12 (2013) 089. [arXiv:1307.3536](#), [doi:10.1007/JHEP12\(2013\)089](#).
- [43] J. Elias-Miro, J. R. Espinosa, T. Konstandin, Taming Infrared Divergences in the Effective Potential, JHEP 08 (2014) 034. [arXiv:1406.2652](#), [doi:10.1007/JHEP08\(2014\)034](#).
- [44] A. Andreassen, W. Frost, M. D. Schwartz, Consistent Use of the Standard Model Effective Potential, Phys. Rev. Lett. 113 (24) (2014) 241801. [arXiv:1408.0292](#), [doi:10.1103/PhysRevLett.113.241801](#).

- [45] N. K. Nielsen, On the Gauge Dependence of Spontaneous Symmetry Breaking in Gauge Theories, Nucl. Phys. B101 (1975) 173. doi:10.1016/0550-3213(75)90301-6.
- [46] F. Bezrukov, M. Yu. Kalmykov, B. A. Kniehl, M. Shaposhnikov, Higgs Boson Mass and New Physics, JHEP 10 (2012) 140. arXiv:1205.2893, doi:10.1007/JHEP10(2012)140.
- [47] S. Alekhin, A. Djouadi, S. Moch, The top quark and Higgs boson masses and the stability of the electroweak vacuum, Phys. Lett. B716 (2012) 214–219. arXiv:1207.0980, doi:10.1016/j.physletb.2012.08.024.
- [48] I. Masina, Higgs boson and top quark masses as tests of electroweak vacuum stability, Phys. Rev. D87 (5) (2013) 053001. arXiv:1209.0393, doi:10.1103/PhysRevD.87.053001.
- [49] P. A. R. Ade, et al., Planck 2015 results. XIII. Cosmological parameters. arXiv:1502.01589.
- [50] K. Allison, Higgs xi-inflation for the 125-126 GeV Higgs: a two-loop analysis, JHEP 1402 (2014) 040. arXiv:1306.6931, doi:10.1007/JHEP02(2014)040.
- [51] A. De Simone, M. P. Hertzberg, F. Wilczek, Running Inflation in the Standard Model, Phys. Lett. B678 (2009) 1–8. arXiv:0812.4946, doi:10.1016/j.physletb.2009.05.054.
- [52] J. Fumagalli, M. Postma, UV (in)sensitivity of Higgs inflation, JHEP 05 (2016) 049. arXiv:1602.07234, doi:10.1007/JHEP05(2016)049.
- [53] A. Barvinsky, A. Y. Kamenshchik, A. Starobinsky, Inflation scenario via the Standard Model Higgs boson and LHC, JCAP 0811 (2008) 021. arXiv:0809.2104, doi:10.1088/1475-7516/2008/11/021.